[1]*Grupo de Herpetología Patagónica, Instituto para el Estudio de los Ecosistemas Patagónicos, IPEEC-CONICET, Puerto Madryn, Chubut, Argentina; [2]Biology Department and Bean Life Science Museum, Brigham Young University, Provo, UT, USA*

Phylogeographic history of Patagonian lizards of the *Liolaemus elongatus* complex (Iguania: Liolaemini) based on mitochondrial and nuclear DNA sequences

CINTIA DÉBORA MEDINA[1], LUCIANO JAVIER AVILA[1], JACK WALTER SITES JR[2] and MARIANA MORANDO[1]

Abstract

In this study, we present a phylogeographic analysis of a group of lizards distributed in north-western Patagonia, the *Liolaemus elongatus* complex. We sequenced 581 individuals for one mitochondrial gene (*cytochrome-b*), and for a subset, we sequenced another mitochondrial gene (*12S rRNA*) and two nuclear genes: *kinesin family member 24* (*KIF24*) and the anonymous nuclear locus *LDAB1D*. We estimated gene trees, mitochondrial and nuclear haploytpe networks, standard molecular diversity indices, genetic distances between lineages and Bayesian skyline plots. Our results provide evidence for recognition of seven species previously described within the *L. elongatus* complex: *Liolaemus antumalguen*, *Liolaemus chillanensis*, *Liolaemus carlosgarini*, *Liolaemus burmeisteri*, *Liolaemus smaug*, *Liolaemus elongatus* and *Liolaemus crandalli*, but we did not find sufficient evidence to support *Liolaemus choique*, *Liolaemus shitan* or *Liolaemus* sp. 6 as distinct species. We identified four candidate species (*Liolaemus* sp. 1, *Liolaemus* sp. 2, *Liolaemus* sp. 3 and *Liolaemus* sp. 7), and we discuss evolutionary processes that may have contributed to the origin of these lineages and their taxonomic and conservation implications.

Key words: North-western Patagonia – *Liolaemus elongatus* complex – phylogeography – divergence time – mitochondrial gene – nuclear gene

Introduction

The lizard genus *Liolaemus* is emerging as a model group for a variety of studies (Breitman et al. 2014), and it includes over 257 currently described species in temperate South America (Abdala and Quinteros 2014). The genus not only is one of the most species-rich temperate terrestrial vertebrate genera, but it is also ecologically very diverse (Harmon et al. 2003; Pincheira-Donoso et al. 2009), and distributed over a wide geographic area that includes climatic regions ranging from the world's driest desert to the humid *Nothofagus* forests (Donoso Barros 1966; Cei 1986, 1993; Lobo et al. 2010). This distribution extends over a latitudinal range of 14–52°S (Etheridge and Espinoza 2000) and altitudes from sea level to almost 5000 m. *Liolaemus* includes two major clades usually referred to as subgenera, *Liolaemus* and *Eulaemus* (Laurent 1983; Etheridge 1995; Schulte et al. 2000; Pincheira-Donoso et al. 2008; Lobo et al. 2010). Within the subgenus *Liolaemus*, also known as the *L. chiliensis* group, several species clades and complexes have been recognized, one of which is the *L. elongatus-kriegi* group that includes the *L. elongatus* Koslowsky, 1896, *L. kriegi* Müller and Hellmich, 1939, and *L. petrophilus* Donoso-Barros and Cei, 1971, complexes (*sensu* Morando et al. 2003).

The *L. elongatus* complex includes species confined to the Patagonian region, which extends latitudinally from 35°06′S to 45°27′S. Morando et al. (2003) found that the nominal species, *Liolaemus elongatus* Koslowsky, 1896, is distributed from southern Mendoza to south-western Chubut and included several related and geographically concordant haploclades [*L.* sp. 5, later described as *Liolaemus smaug* Abdala, Quinteros, Scrocchi and Stazzonelli, 2010; (Abdala et al. 2010), *Liolaemus* sp. 6, *Liolaemus* sp. 7 and *Liolaemus elongatus sensu stricto*]. Several subsequent studies (Torres-Pérez et al. 2009; Abdala et al. 2010;

Avila et al. 2010, 2012, 2015; Esquerré et al. 2013) have considered or suggested as part of this complex up to eight additional species: *Liolaemus chillanensis* Müller and Hellmich, 1932, *Liolaemus burmeisteri* Avila, Perez, Medina, Sites and Morando, 2012; *Liolaemus shitan* Abdala, Quinteros, Scrocchi and Stazzonelli, 2010; *Liolaemus choique* Abdala, Quinteros, Scrocchi and Stazzonelli, 2010; *Liolaemus smaug*, *Liolaemus crandalli* Avila, Medina, Perez, Sites and Morando, 2015; *Liolaemus antumalguen* Avila, Morando, Perez and Sites, 2010; and *Liolaemus carlosgarini* Esquerré, Núñez and Scolaro, 2013; the majority of these have been described in the last decade.

The geographic distributions of the described and candidate species of the *L. elongatus* complex overlap in several localities (Fig. 1), and taxonomic identifications are ambiguous. One particular case is *L. parvus* Quinteros, Abdala, Gómez and Scrocchi, 2008, which was described on the basis of morphological characters, and hypothesized by some to be part of the *L. capillitas* Hulse, 1979 clade (Díaz Gómez and Lobo 2006). This clade is considered to be part of the *L. petrophilus* complex, but phenotypically, it is more similar to *L. elongatus* than to the other species in this complex. Furthermore, studies based on nuclear and mitochondrial sequences inferred *L. parvus* within the *L. petrophilus* complex (Morando et al. 2003; Avila et al. 2004; Feltrin 2013). These contradictions highlight the point that species boundaries within the *L. elongatus* complex, and their phylogenetic relationships, are limited and have not advanced much beyond the original phylogeographic study published more than a decade ago (Morando et al. 2003).

This complex inhabits north-western Patagonia, a geographically complex region characterized by mountains up to 4500 m, large volcanic fields, deep canyons and high plateaus. These features are the products of an Andean orogenic history that includes sporadic volcanic eruptions and cyclic glacial advances and retreats that produced pronounced climatic changes throughout the last myr (Rabassa and Clapperton 1990; Ramos and Kay 2006; Ramos and Ghiglione 2008; Martínez and Kutschker 2011; Ramos and Folguera 2011). As a result, this climate history superimposed on a complex topography likely fostered multiple population-divergence processes across different

Corresponding author: Cintia Débora Medina (medina@cenpat-conicet.gob.ar)
Contributing authors: Luciano Javier Avila (avila@cenpat-conicet.gob.ar), Jack Walter Sites (jack_sites@byu.edu), Mariana Morando (morando@cenpat-conicet.gob.ar)
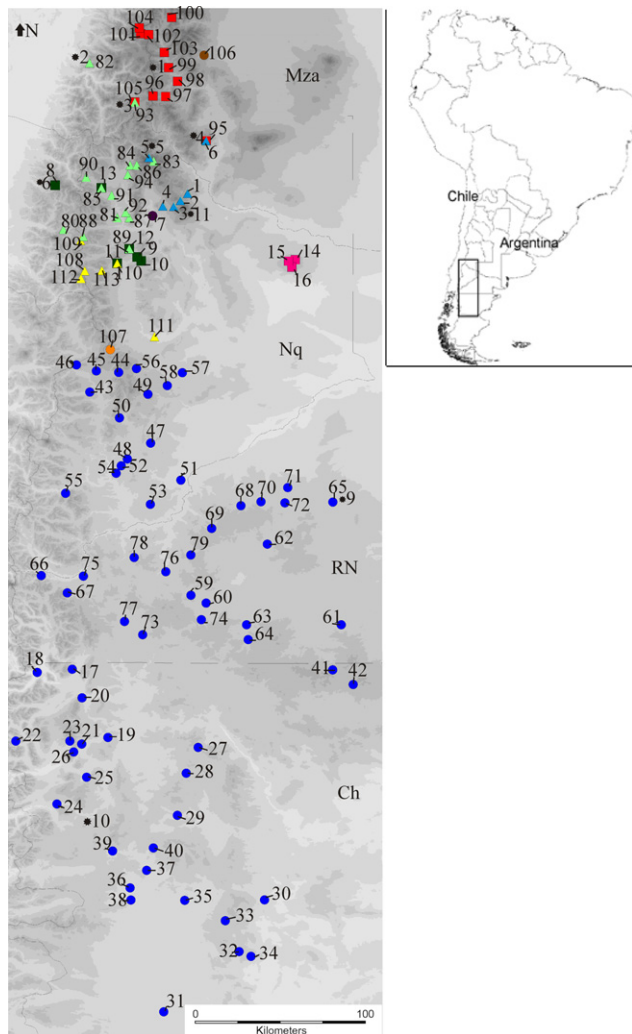
Fig. 1. Localities sampled for the *L. elongatus* complex as follows: *L. antumalguen* + *L.* sp. 7, blue triangles (1 6); *L. burmeisteri*, purple circle (7); *L. chillanensis*, dark green squares (8 13); *L. crandalli*, pink squares (14 16); *L. elongatus* + *L. shitan*, blue circles (17 79); *L. carlosgarini* + *L.* sp. 1, light green triangles (80 94); *L. smaug*, red squares (95 105); *L.* sp. 2, brown circle (106); *L.* sp. 3, orange circle (107); *L.* sp. 6, yellow triangles (108 113). Although we sampled the type locality of *L. choique* [*4], these individuals are genetically related to *L. antumalguen* and *L. smaug*; thus, we do not have a colour code for this species on this map. Ch, Chubut Province, Nq, Neuquén Province, Mza, Mendoza Province and RN, Río Negro Province. The numbers correspond to those given in Table S1 (Colours match those given in Figs. 3 and 4). Type localities or candidates species localities appear identified with an asterisk: *1 – *L. smaug*, *2 – *L.* sp. 1, *3 – *L. carlosgarini*, *4 – *L. choique*, *5 – *L. antumalguen*, *6 – *L. chillanensis*, *9 – *L. shitan*, *10 – *L. elongatus* (this type locality is 'territorio del oeste de Chubut', thus the position of this asterisk is approximate) and *11- *L.* sp. 7.

geographical and temporal scales (Morando et al. 2013), which may explain the unusually high number of lizard biodiversity in this region (Corbalán et al. 2011; Avila et al. 2013a). As an example, several new species of lizards from this and other genera were recently described from this area (Abdala et al. 2012a, b; Avila et al. 2012, 2013b, 2015; Lobo and Nenda 2015), and several new candidate species have been identified (Medina et al. 2013; Olave et al. 2017). The most boreal area of this region, corresponding to northern Neuquén Province (Fig. 1), has been identified as a biodiversity 'hot spot' due to high levels of endemism in South American beetle species (Carabidae, Casagranda

et al. 2009; Domínguez et al. 2006), as well as a high percentage of priority and irreplaceable Patagonian conservation areas (Chehébar et al. 2013). These earlier studies lead to predictions of a high number of lizard species for this region (Corbalán et al. 2011; Avila et al. 2013a). Therefore, we expect to find a higher number of haploclades than in previously published phylogenies.

The main goal of this study was to use molecular data to examine the phylogenetic/phylogeographic structure and patterns of variation in the *L. elongatus* complex, based on samples from throughout its known distributional range. We included 12 taxa: nine described species (*L. chillanensis*, *L. antumalguen*, *L. burmeisteri*, *L. smaug*, *L. carlosgarini*, *L. elongatus*, *L. shitan*, *L. choique* and *L. crandalli*), one being described (*L.* sp. 1, Esquerré, personal communication) and two candidate species (*L.* sp. 6 and *L.* sp. 7, Morando et al. 2003).

Materials and Methods

Sampling

We sampled 113 localities that cover the known distributional range of the *L. elongatus* complex, from southern Mendoza (35°11′S) to southern Chubut (45°71′S) provinces in Argentina, and six localities from a small range in Chile (Fig. 1), from which we obtained 581 individuals. To test the proposal that *L. parvus* could be part of this complex, we also included individuals from its type locality, 58 km west of Jagüe, General Sarmiento Department, La Rioja Province, Argentina. Table S1 includes specimen voucher numbers with localities details. We collected specimens by hand and euthanized them with a pericardial injection of sodium pentothal. We took liver samples and stored these in 96% ethanol, fixed specimens in 20% formalin, and later transferred these to 70% ethanol. Voucher specimens and tissues are deposited on the herpetological collection LJAMM-CNP housed at the Instituto Patagónico para el Estudio de los Ecosistemas Continentales (IPEEC), Centro Nacional Patagónico (CENPAT-CONICET) in Puerto Madryn, Argentina (http://www.cenpat.edu.ar/nuevo/colecciones03.html). We also included seven tissue samples from the personal collection of Miguel I. Christie (MIC), including six samples of *L. petrophilus*, *L. buergeri* and *L. tregenzai* Pincheira-Donoso and Scolaro, 2007, that represent phylogenetically closely related groups, and a sample of *L. bibronii* (Bell, 1843) to root the tree. Sequences determined in this study are deposited in GenBank under the accession numbers KY127454–KY128171. For each species, specimen voucher number, haplotype details and GenBank accession numbers are listed in Tables S2 and S3.

DNA extraction, amplification and sequencing

We extracted DNA using Qiagen DNeasy® tissue kits (Qiagen Inc., Valencia, CA) following the protocol provided by the manufacturer. We sequenced two mitochondrial gene sections (*12S rRNA* [*12S*, 856 bp, 71 individuals] and *cytochrome-b* [*cyt-b*, 675 bp, 581 individuals]) and two nuclear gene sections [a member of the kinesin family 24 (*KIF24*, 417 bp, 56 individuals, Portik et al. 2011) and an anonymous nuclear gene *LDAB1D* (*LDAB1D*, 511 bp, 46 individuals, Camargo et al. 2012a)]. For PCR and sequencing protocols, we followed Morando et al. (2003, 2004) and Noonan and Yoder (2009) for mitochondrial and nuclear genes, respectively. PCR protocol for mitochondrial genes: 94°C–3 min; 40× [94°C–1 min, 45°C–1 min, 72°C–1 min]; 72°C–7 min; 4°C – forever. For nuclear genes, the protocol is a standard touch-down cycle: 95°C–1.5 min; 10× [95°C–35 s, 63°C–35 s (−0.5°C/cycle), 72°C–1 min]; 10× (95°C–35 s, 58°C–35 s, 72°C–1 min); 15× (95°C–35s, 52°C–35s, 72°C–1 min); 72–10 min. For nuclear and mitochondrial genes, we set up standard PCR reaction conditions: 1.0 μl of template DNA, 2 μl dNTPs (1.25 mM), 2 μl 10× Taq buffer, 1 μl of each primer (10 μM), 1 μl MgCl (25 mM), 6.5 μl distilled water and 0.1 μl Taq DNA polymerase (5 U/μl; Promega Corp., Madison, WI). Primer sequences: *cyt-b* gene, two forward primers, GLUDGL (5′-TGACTTG AARAACCAYCGTTG-3′) and *cyt-b* 1 (5′-CCATCCAACATCTCAGCA TGATGAAA-3′) and the heavy strand primer CHB-3 (5′-GGCAAAT AGGAARTATCATTC-3′). *12S* gene, 12e (5′-GTRCGCTTACC W

TGTTACGACT-3′) and tPhe (5′-AAAGCACRGCACTGAAGATGC-3′). *KIF24* gene, F1 (5′-SAAACGTRTCTCCMAAACGCATCC-3′) and R1 (5′-WGGCTGCTGRAAYTGCTGGTG-3′). *LDAB1D* gene, B1D F (5′-GATATCGAGGGATTTCAGTTTCC3′) and B1D R (5′-CCAGTGTT TATGAGCAACTGAGTA-3′). Double-stranded PCR amplified products were checked by electrophoresis on a 2% agarose gel, purified using a Multi-Screen PCR (l) 96 (Millipore Corp., Billerica, MA), and directly sequenced using the BigDye Terminator v 3.1 Cycle Sequencing Ready Reaction (Applied Biosystems, Foster City, CA). The cycle sequencing reactions were purified using Sephadex G-50 Fine (GE Healthcare) and MultiScreen HV plates (Millipore Corp.). Samples were then analysed on an ABI3730xl DNA Analyzer in the BYU DNA Sequencing Center. We used Sequencher v4.10. (Gene Codes Corporation Inc.™ 2007) to edit and align all the genes, we also translated to protein to verify for stop codons and alignments were checked by eye. Alignments available at TreeBASE, http://purl.org/phylo/treebase/phylows/study/TB2:S20311).

We sequenced the *cyt-b* for all the 581 individuals, and based on the inferred *cyt-b* gene tree, we selected a subsample that included at least two representatives of each haploclade on the tree, for which we sequenced the mitochondrial *12S* gene and the two nuclear markers. We used the complete *cyt-b* matrix for all of the phylogeographic analyses; we used the other three markers to infer single-locus networks and a combined multilocus network for both nuclear genes.

Gene tree analysis and networks

Before we ran the concatenated analyses, we evaluated different codon partitions for the *cyt-b* gene through Bayesian factor analysis (Kass and Raftery 1995) on MrBayes v3.2 (Ronquist and Huelsenbeck 2003). The first model we tested was an unpartitioned model, and the second one was partitioned by codon. For both models, we ran 10 million generations with their respective selected molecular evolution models. Based on these results, we used a matrix with partitioned *cyt-b*. To infer a *cyt-b* gene tree, we selected non-redundant haplotypes with DnaSP 5.10 (Librado and Rozas 2009), and estimated a gene tree with a Bayesian inference (BI) method. We used JModelTest v2.1.7 (Guindon and Gascuel 2003; Darriba et al. 2012) to select the evolutionary model that best fits each *cyt-b* gene partition, using the corrected Akaike information criterion (AICc). We ran MrBayes v3.2 (Ronquist and Huelsenbeck 2003) for 5×10^7 generations, and used equilibrium samples (after 25% burnin) to generate a 50% majority rule consensus tree; we considered posterior probabilities (PP) significant when ≥0.95 (Huelsenbeck and Ronquist 2001). To name lineages within the *L. elongatus* complex, we identified haploclades that included individuals from type localities of the described species, and haploclades that included individuals from the localities assigned to candidate species by Morando et al. (2003). We used the *cyt-b* and *12S* matrices and the *KIF24* and *LDAB1D* nuclear genes (previously phased with the program phase which is built into DnaSP with the default settings; Librado and Rozas 2009) to infer statistical parsimony networks with the 95% probability criteria using TCS 1.21 (Clement et al. 2000). We also used a nuclear distance matrix to generate a multilocus network using POFAD v1.03 (Joly and Bruneau 2006) and visualized the reconstruction of the organism network using the NeighborNet algorithm implemented in SplitTrees v4.6 (Huson and Bryant 2005) following Leaché et al. (2009). We also constructed a mtDNA network (both genes combined) with the 95% probability criterion as implemented in TCS 1.21. We tested recombination for nuclear genes regions using the RDP program v3.44 (Martin and Rybicki 2000; Heath et al. 2006).

Phylogeographic analysis

We used Arlequin v3.1 (Excoffier et al. 2005) to calculate genetic distances (corrected and uncorrected in pairs) between the different lineages inferred in the gene trees. To generate a first round of candidate species hypotheses, we followed the criteria described by Fouquet et al. (2007) which consider a lineage specific genetic distance threshold above which species may be different in combination with allopatric distributions. Based on genetic distances of formerly described species based on morphology and following Martínez (2012) and Breitman et al. (2012) methodology, we calculated specific uncorrected pairwise distances of *cyt-b*, which on average was 4% for pairwise comparisons [other *Liolaemus* estimates: 4% in Martínez (2012) and 3% in Breitman et al. (2012)]. Here, we identified haploclades with pairwise genetic distances greater than 4% and from geographically isolated areas as candidate species. We used the partitioned *cyt-b* matrix to estimate divergence times among major lineages, with their best-fit models of molecular evolution identified by JModeltest v2.1.7 (Guindon and Gascuel 2003; Darriba et al. 2012), and performed likelihood ratio tests (LRT) implemented in the program HYPHY (Pond and Muse 2005) to evaluate deviations from a strict molecular clock. We used the Fontanella et al. (2012) *cyt-b* evolutionary rate of 2.23-2, as estimated for the *Eulaemus* clade calibrated with the only known *Liolaemus* fossil. We then used BEASTv1.8.1 to estimate the gene tree under a relaxed molecular clock model (Drummond and Rambaut 2007). We performed two independent analyses for 100 million generations, sampled every 1000 generations, under a GTR + G nucleotide substitution model for the 1st position and GTR + G + I for the 2nd and 3rd, and assuming a prior Yule tree. We verified the effective sample size (ESS) for parameter estimates and convergence using Tracer v1.6 (Rambaut and Drummond 2009).

Demographic analysis

We estimated standard molecular diversity indices: number of sequences (NS), polymorphic sites (S), haplotypes (H), haplotype diversity (Hd) and nucleotide diversity (Pi), for each of the major haploclades inferred from the mitochondrial gene tree, and for these combined lineages: *L. antumalguen* + *L. chillanensis* + *L.* sp. 6a + *L.* sp. 6b (see Results). We performed Tajima neutrality tests (Tajima 1989) and Ramos-Onsins and Rozas tests (Ramos-Onsins and Rozas 2002) to evaluate possible temporal changes in population size, using the DnaSP program. We also estimated Bayesian skyline plot (BSP) to model ESS changes over time, for *L. antumalguen* + *L.* sp. 7, *L. chillanensis*, *L. carlosgarini* + *L.* sp. 1, *L. smaug*, *L. elongatus* + *L. shitan* and *L. crandalli*. We used a relaxed molecular clock and a specific model of molecular evolution for each lineage, ran 2×10^7 iterations, sampled each 1000 iterations and analysed convergence of the parameters with the program Tracer v1.5 (Rambaut and Drummond 2009). These analyses were not performed for other lineages due to small sample sizes.

Results

Analysis of gene trees and networks

From 581 *cyt-b* sequences obtained for the *L. elongatus* complex, we found 249 non-redundant haplotypes. The best-fit nucleotide substitution models were GTR + G (1st position), GTR + I + G (2nd position) and TPM1uf + I (3rd position), and based on the PartitionFinder results, we combined 2nd and 3rd positions to infer a *cyt-b* gene tree for this group for which we obtained high support (posterior probability [PP] = 1, Fig. 2). We resolved 11 haploclades with high support within this complex, including four described species, *L. chillanensis*, *L. burmeisteri*, *L. smaug* and *L. crandalli*, and in two cases described species were inferred with paraphyletic relationships with candidate species: *L. carlosgarini* included *L.* sp. 1 haplotypes and *L. antumalguen* included *L.* sp. 7 haplotypes. We inferred two lineages that we designate as candidate species *L.* sp. 2 and *L.* sp. 3, and two lineages corresponding to a candidate species previously identified as *L.* sp. 6 by Morando et al. (2003), that we identify as *L.* sp. 6a and *L.* sp. 6b. The last haploclade corresponds to *L. elongatus*, but it includes four haplotypes found among 35 individuals from the type locality of *L. shitan*; thus, this haploclade was named (*L. elongatus* + *L. shitan*).

Other individuals assigned to *L. shitan* (based on coloration and geographical proximity) from localities 71 (two individuals) and 68 and surroundings (4 individuals) were placed outside of the *L. elongatus* complex in two different regions of the tree (Fig. 2). Note that other individuals from the same area had

Fig. 2. Bayesian 50% majority rule consensus *cyt-b* gene tree. The numbers above branches are posterior probability values. Asterisks with numbers within *L. antumalguen* + *L.* sp. 7 and *L. smaug* haploclades represent the number of individuals of *L. choique* recovered in each of them.

haplotypes that were included within the *L. elongatus* + *L. shitan* haploclade (see Table S2). Based on this result, we did not include the six individuals placed external to this complex in subsequent analyses. The haplotypes of the six individuals collected at the type locality of *L. choique* (Fig. 1, localities 6/95) were inferred in two other species haploclades, two within *L. antumalguen* and four within *L. smaug* (asterisks inside triangles followed by 2 and 4 in Fig. 2).

Relationships among the 11 haploclades were mostly unresolved, but we resolved three clades with high support (PP = 1): ((*L. elongatus* + *L. shitan*) + *L.* sp. 3); (*L. antumalguen*, *L. chillanensis*, *L.* sp. 6a, *L.* sp. 6b); and ((*L. antumalguen*, *L. chillanensis*, *L.* sp. 6a, *L.* sp. 6b) + *L. carlosgarini*). *Liolaemus* sp. 6 was previously proposed as a candidate species (Morando et al. 2003), and this same identity we give it here (*L.* sp. 6a and *L.* sp. 6b), as we also name *L.* sp. 2 and *L.* sp. 3, and they are not an endorsement of their recognition as distinct species; we simply use the label 'candidate species' as hypotheses that require further comprehensive studies to assess their taxonomic status.

The general results of our *cyt-b* network analysis (Fig. 3) are consistent with the gene tree (Fig. 2). We obtained separate networks for *L.* sp. 2 (Fig. 3, panel d), *L.* sp. 3 (Fig. 3, panel e), *L. burmeisteri* (Fig. 3, panel f) and *L. crandalli* (Fig. 3, panel i). Haplotypes corresponding to the *L. carlosgarini* + *L.* sp. 1 haploclade (Fig. 2), formed two separate networks; one included the

two haplotypes from the type locality of *L.* sp. 1 (Fig. 1, loc. *2); and the second network corresponds to *L. carlosgarini* (Fig. 1, loc. *3). The *L. smaug* network (Fig. 3, panel b) identifies haplotypes from the *L. smaug* type locality (dark green circle and a black *1) and included the following: 1 – one terminal haplotype shared among five individuals from the type locality of *L. carlosgarini* (Fig. 3, panel b) and 2 – one terminal haplotype shared between four individuals from the type locality of *L. choique* (Fig. 3, panel b, blue circle with a red *4). The network that included *L. antumalguen* and *L. chillanensis* (Fig. 3, panel g, haplotypes from individuals of the type locality of *L. antumalguen* are identified with a pink circle and black star and those from the type locality of *L. chillanensis* with a violet circle and a black star), also included an haplotype shared by two individuals of the type locality of *L. choique* (Fig. 1, loc. *4; Fig. 3, panel g, blue circle with a red *4). Therefore, the six individuals collected in the type locality of *L. choique* (Fig. 1, loc. *4) were inferred in two different networks, two in *L. antumalguen* + *L. chillanensis* (Fig. 3, panel g, red *4) and four within *L. smaug* (Fig. 3, panel b, red *4). The *L. antumalguen* + *L. chillanensis* network (Fig. 3, panel g) shows that the three haplotypes found in nine individuals from the type locality of *L. antumalguen* (Fig. 3, panel g, three pink circles with black star, within the blue shaded area) only differ on one base pair, and the other 32 haplotypes on the network (from 65 individuals collected at four localities) correspond to *L.* sp. 7
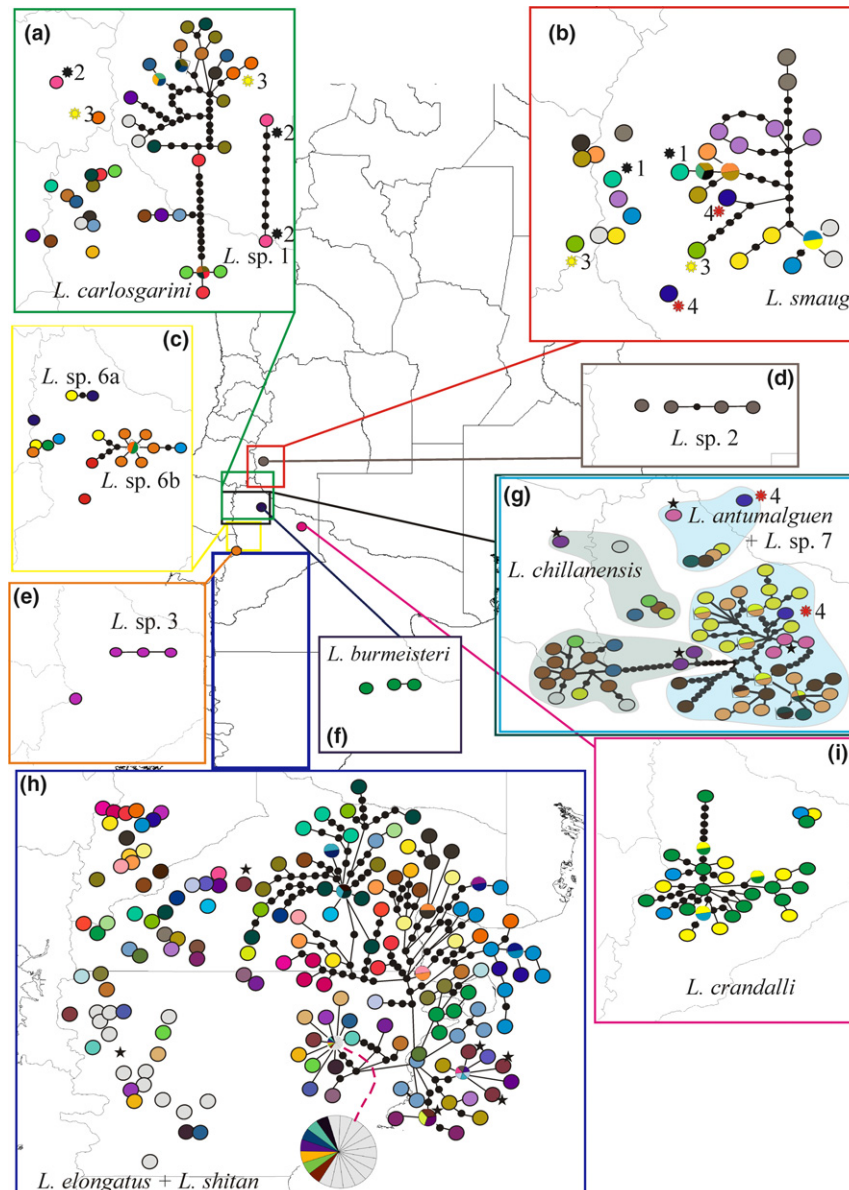
Fig. 3. Panels a to i show statistical parsimony haplotype *cyt-b* gene networks. Each lineage appears with its respective geographical distribution and each haplotype is colour-coded according to its geographical distribution. a – *L. carlosgarini*; b – *L. smaug*; c – *L.* sp. 6 (a and b); d – *L.* sp. 2; e – *L.* sp. 3; f – *L. burmeisteri*; g – *L. chillanensis* (grey shaded) and *L. antumalguen* + *L.* sp. 7 (blue shaded); h – *L. elongatus* + *L. shitan* and i – *L. crandalli*. Red asterisk of panels b and g mark the type locality of *L. choique*. The yellow asterisk of panels a and b mark the type locality of *L. carlosgarini*. The black asterisk represents the type localities of: a – *L.* sp. 1, b – *L. smaug*. In panels g and h, stars represent type localities of *L. chillanensis* and *L. antumalguen* and *L. elongatus* and *L. shitan,* respectively. Black spots within networks represent mutational steps.

(Fig. 1, locs. 1 to 4). Within the same network (Fig. 3, panel g), separated by 10 mutational steps, are the haplotypes corresponding to *L. chillanensis* (grey shaded area, two purple circles with a black star correspond to those from the type locality).

The two *L.* sp. 6 haploclades on the mitochondrial tree (Fig. 2) were placed in two separate networks (Fig. 3, panel c), one in *L.* sp. 6a and the other in *L.* sp. 6b. The network *L.* sp. 6a includes two haplotypes, one from a northern locality and the others from localities in the south (Fig. 3, panel c, blue and yellow circles). The network *L.* sp. 6b includes haplotypes of the rest of the localities in the south plus one haplotype from the same locality also inferred as part of the *L.* sp. 6a network (Fig. 3, panel c, yellow circle).

The network in panel H (Fig. 3) represents haplotypes from the distributions of both *L. elongatus* and *L. shitan*, and while

individuals from the type locality of *L. shitan* (Fig. 3, panel h, purple circle with black star) are not shared with individuals of *L. elongatus*, they are only separated by one mutational step.

We obtained one network with the *12S* sequences (Fig. 4, panel a) that shows colour-coded the haploclades identified with the *cyt-b* gene (Figs. 2 and 3). The two mitochondrial gene networks (Figs. 3 and 4a) are completely consistent with the combined mitochondrial gene network (Fig. S1). The nuclear network obtained with the *KIF24* gene had a connection limit of eight steps (Fig. 4, panel c), and the singleton that corresponds to *L. burmeisteri* was placed outside of this network. Most nuclear haplotypes are species-specific, but with some exceptions: two haplotypes are shared between *L. elongatus* and *L. antumalguen*, a third haplotype is shared between *L. smaug* and *L. carlosgarini*, and a fourth haplotype is shared among four
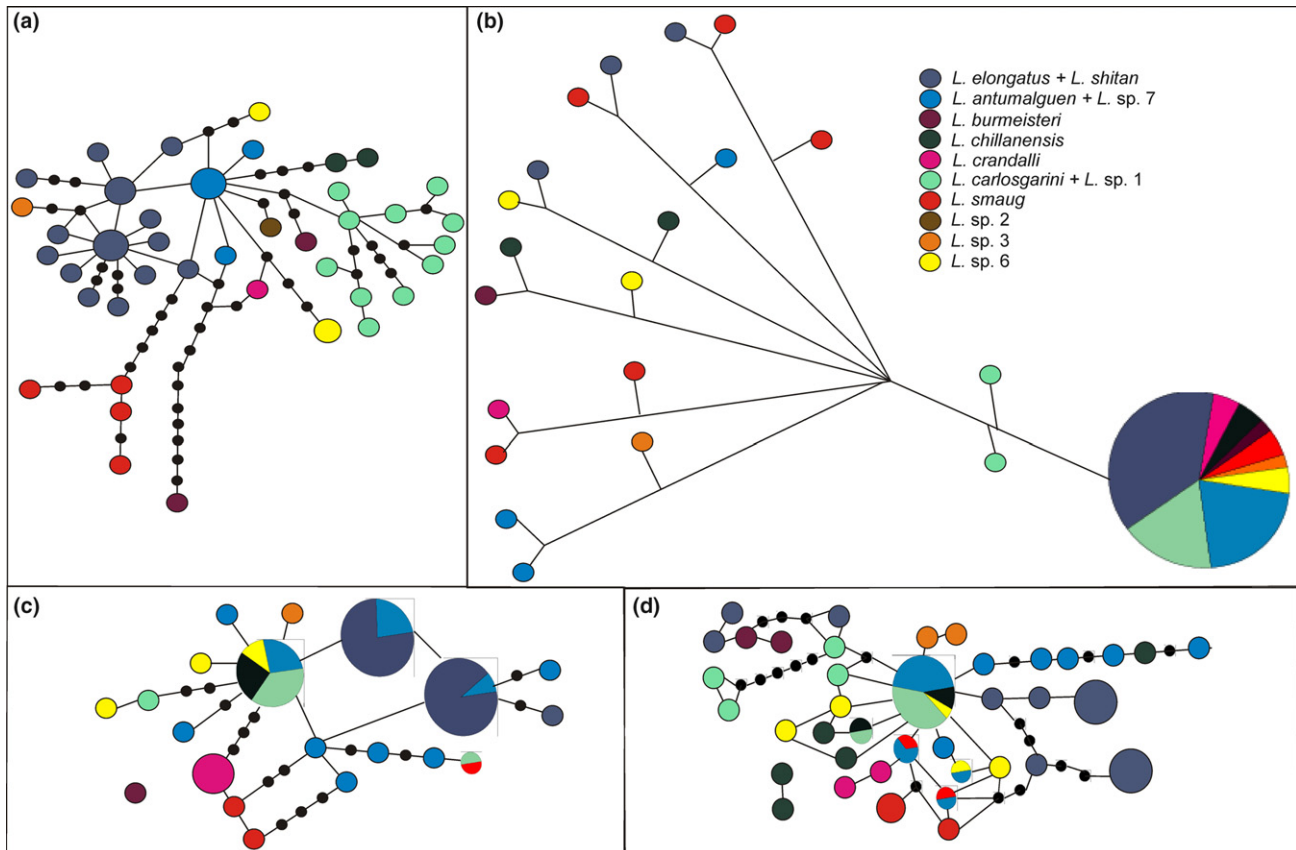
Fig. 4. Statistical parsimony haplotype networks based on: a – the mitochondrial *12S* region; b – the nuclear multilocus network (*LDAB1D* y *KIF24*); c – the *KIF24* network; and d – the *LDAB1D* network. Haplotypes are colour-coded for each recognized lineage within the *L. elongatus* complex. Black spots within networks represent mutational steps.

taxa: *L. carlosgarini*, *L. antumalguen*, *L. chillanensis* and *L.* sp. 6.

The nuclear *LDAB1D* network had a nine-step connection limit (Fig. 4, panel d), and as above showed that most of the haplotypes are species-specific, but with exceptions. Two haplotypes are shared between *L. smaug* and *L. antumalguen*, and the remaining three are shared among the following taxa: 1 – *L. chillanensis* and *L. carlosgarini*, 2 – *L.* sp. 6 and *L. antumalguen*, 3 – *L. antumalguen*, *L. carlosgarini*, *L.* sp. 6 and *L. chillanensis*. The two-locus network summarizes average genetic distances among individuals (Fig. 4, panel b); we found that almost all taxa, except *L. burmeisteri*, have equal distances between them (large circle with nine colours), while other individuals of a subset of taxa have shorter distances (e.g. *L. antumalguen*, blue circles in the lower right corner).

Phylogeographic analysis

Table 1 shows the 51 pairwise uncorrected genetic distances for the 11 haploclades recognized within the *L. elongatus* complex (Fig. 2). Most of the distances are greater than 4%, but with 10 exceptions (note that three of them are very close to 4%): *L. chillanensis* vs. *L. antumalguen* (2.7%), *L.* sp. 3 vs. (*L. elongatus* + *L. shitan*) (2.93%), *L. carlosgarini* vs. *L. antumalguen* (3.23%), *L. carlosgarini* vs. *L. chillanensis* (3.34%), *L.* sp. 6a vs. *L. chillanensis* (3.02%), *L.* sp. 6b vs. *L. chillanensis* (3.11%), *L.* sp. 3 vs. *L. crandalli* (3.92%), *L.* sp. 6a. vs. *L. carlosgarini* (3.58%), *L.* sp. 6b vs. *L. carlosgarini* (3.69%) and *L.* sp. 6a vs. *L.* sp. 6b (2.96%). The taxon with the largest genetic distance was *L. smaug* (>5% in all pairwise comparisons; min: 5.04, max: 6.20).

The time calibrated *cyt-b* gene tree (Fig. 5) places the origin of *L. elongatus* complex at 2.2–3.3 million years ago, during the late Pliocene, and most of the other divergence times within the complex are estimated within the Pleistocene.

Demographic analysis

Liolaemus sp. 6a had the fewest sequences, polymorphic sites, haplotypes and the lowest haplotype diversity (Table 2). The (*L. elongatus* + *L. shitan*) clade had the largest sample size, and the highest number of polymorphic sites and haplotypes. *Liolaemus crandalli* and the clade (*L. antumalguen*, *L. chillanensis*, *L.* sp. 6a and *L.* sp. 6b) had the highest haplotype diversity, and *L. burmeisteri* had the highest nucleotide diversity. The only taxa that showed evidence of non-neutrality with both the Tajima's and Onsins and Rozas tests were (*L. elongatus* + *L. shitan*) and *L. crandalli*. *Liolaemus chillanensis* was inferred to be non-neutral with the Tajima test. The Bayesian skyline plot (BSP) analyses detected a change in population sizes for all lineages, the most pronounced for (*L. elongatus* + *L. shitan*) (Fig. S2).

Discussion

The aim of this work was to estimate the phylogeographic structure of the *L. elongatus* lizard complex, based on mitochondrial and nuclear markers, and including individuals from throughout its known geographic distribution, as well as the type locality of the hypothesized closely related species *L. parvus*. The mitochondrial *cyt-b* gene tree (Fig. 2) inferred 11 major haploclades, six of which can be assigned to described species

Table 1. Pairwise genetic differences between the eleven recognized lineages of the *L. elongatus* complex. Above diagonal: Average number of pairwise differences corresponding to the *cyt-b* gene between lineages of *Liolaemus*; below diagonal: corrected average pairwise differences (interlineage distance – intralineage distance).

Lineages	*L. antumalguen* + *L.* sp. 7	*L. burmeisteri*	*L. chillanensis*	*L. crandalli*	*L. elongatus* + *L. shitan*	*L. carlosgarini* + *L.* sp. 1	*L. smaug*	*L.* sp. 2	*L.* sp. 3	*L.* sp. 6a	*L.* sp. 6b
L. antumalguen + *L.* sp. 7	—	4.8656	2.7016	5.1426	4.3119	3.2355	5.0434	4.4839	3.4807	2.9206	3.0998
L. burmeisteri	4.0618	—	5.3481	5.3244	5.5155	5.1957	5.7660	4.9629	4.3209	5.1111	5.6378
L. chillanensis	1.5769	4.8790	—	4.9659	4.7571	3.3449	5.2532	4.8757	4.1777	3.0222	3.1111
L. crandalli	3.9930	4.8303	4.1508	—	4.8773	5.0249	5.3236	5.5232	3.9209	5.6118	4.9534
L. elongatus + *L. shitan*	2.7367	4.5959	3.5165	3.6118	—	4.7676	6.2042	5.6335	2.9303	5.0644	4.8638
L. carlosgarini + *L.* sp. 1	1.4713	4.0872	1.9154	3.5704	2.8876	—	5.5555	4.3985	4.0052	3.5873	3.6995
L. smaug	3.6541	5.0322	4.1984	4.2439	4.6989	3.8613	—	5.0838	5.1565	6.0896	5.7760
L. sp. 2	3.6061	4.7407	4.3325	5.2550	4.6399	3.2159	4.2759	—	4.1975	4.9382	5.2016
L. sp. 3	2.7017	4.1975	3.7333	3.4516	2.0354	2.9214	4.4474	4.0000	—	4.6913	4.0768
L. sp. 6a	2.0428	4.8888	2.4790	5.0437	4.0707	2.4046	5.2817	4.6419	4.4938	—	2.9629
L. sp. 6b	2.1397	5.3333	2.4855	4.3029	3.7878	2.4346	4.8858	4.8230	3.7969	2.5843	—

(*L. antumalguen*, *L. chillanensis*, *L. carlosgarini*, *L. burmeisteri*, *L. smaug* and *L. crandalli*), as well as the following: (1) one haploclade included all of the *L. elongatus* samples interdigitated with some from *L. shitan*; (2) two haploclades corresponded to candidate species *L.* sp. 2 and *L.* sp. 3; (3) *L.* sp. 6 individuals were inferred in two different haploclades; (4) the *L. carlosgarini* haploclade also included individuals of *L.* sp. 1; and (5) the *L. antumalguen* haploclade included individuals of *L.* sp. 7 identified by Morando et al. (2003).

Phylogeographic history

The northernmost distributed haploclade in the *L. elongatus* complex is *L. smaug*, with localities in Argentina (Mendoza Province) and Chile north of the Colorado River (Fig. 1, red squares). We did not infer a reciprocally monophyletic relationship between *L. smaug* and three other species, rather the *L. smaug* haploclade includes individuals from three type localities: (1) *L. smaug* in Malargüe, Mendoza (Fig. 1, loc. *1); (2) *L. carlosgarini* in Region VII in Chile (Fig. 1, loc. *3 [locs. 93/105]); and (3) *L. choique* (Fig. 1, loc. *4 [locs. 6/95]). We discuss this result in combination with the network depicted in Fig. 3, panel g that also included haplotypes from the *L. choique* type locality.

The *cyt-b* haplotype network (Fig. 3, panel b) is structured; the two haplotypes from the type localities of *L. carlosgarini* and *L. smaug* both have terminal positions (red *4 and black *1) and are from close geographic areas; thus, current or recent gene flow or incomplete lineage sorting (ILS) may explain this pattern. In the nuclear networks, although most haplotypes are exclusive of *L. smaug*, some are shared with other species; haplotypes from *L. smaug* type locality are shared with haplotypes from the type locality of *L. carlosgarini* (Fig. 1, localities *1 and *3, respectively). The Bayesian skyline plot (BSP) analysis of *L. smaug* suggests a recent slight increase in the effective population size (Fig. S2) that, given the geographic proximity between the type localities of *L. smaug* and *L. carlosgarini* (Fig. 1, locs. *1 and *3), suggests a history of gene flow between these species. In the *KIF24* network (Fig. 4, panel d), haplotypes from the distribution range of *L. smaug* (including haplotypes from *L. choique* type locality, Fig. 1, loc. *4) are shared (Fig. 4, panel D, red and blue circles) with individuals from localities 1, 3 and 4 (Fig. 1, blue triangles located south of the Colorado River) of the *L. antumalguen* haploclade. Given that the time of origin of the ancestor of this haploclade was estimated about half a million years ago, reciprocal monophyly is not expected for most nuclear markers. Further, the Colorado River has been hypothesized as a barrier to gene flow for lizards (Morando et al. 2007) and several other taxa (Sérsic et al. 2011), and if in this context gene flow between *L. smaug* and *L. antumalguen* is not likely, then shared nuclear haplotypes between them may result from incomplete lineage sorting. The *L. smaug* haploclade had the highest pairwise *cyt-b* distances (Table 1), and relatively high haplotype and nucleotide diversities with no statistically detected deviation from neutrality or range expansion (Table 2). This evidence suggests a history of population stability, consistent with the findings for other species of lizards in this geographic region (Morando et al. 2007; Olave et al. 2011; Medina et al. 2014).

The second haploclade distributed north of the Colorado River, is *L.* sp. 2 (Fig. 1, loc. 106), represented by a separate network with three haplotypes from one locality (Fig. 3, panel d) east of the known distribution of *L. smaug*. In the *cyt-b* tree (Fig. 2) *L.* sp. 2 was inferred as monophyletic (PP = 1) and differentiated from the other lineages of the *L. elongatus* complex.
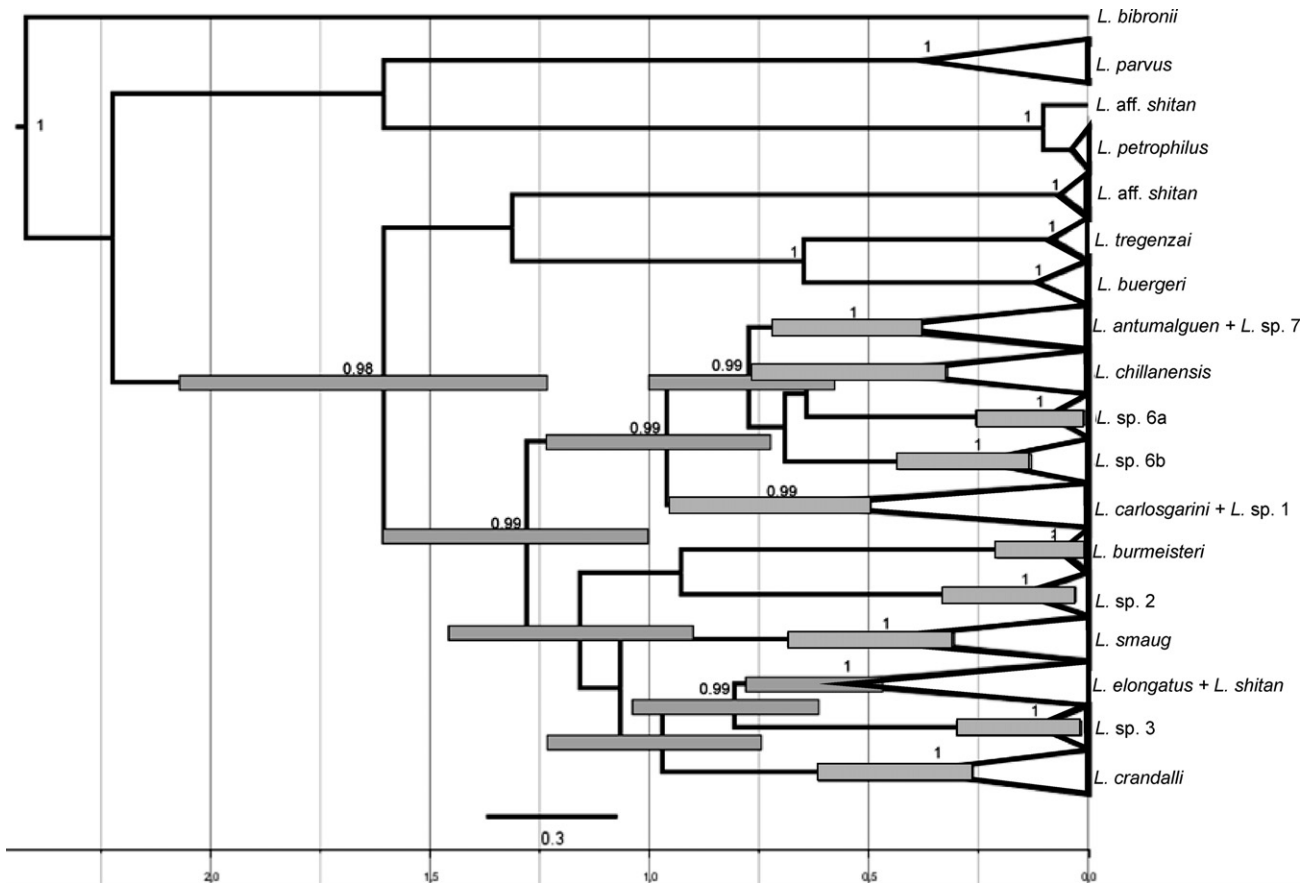
Fig. 5. Estimated divergence times on the *cyt-b* gene tree, marked with light grey, based on BEAST analyses. The *x*-axis is in millions of years (Myr) and numbers on nodes are PP > 0.95 from the Bayesian analysis

Table 2. Demographic analyses of the eleven recognized lineages within the *L. elongatus* complex. All statistics (Tajima's D and associated p values, Ramos-Onsins and Rozas' R^2 and associated p values) were calculated from a fragment of the *cyt-b* mitochondrial gene. H, haplotypes; Hd, haplotype diversity; NS, number of sequences; Pi, nucleotide diversity; S, polymorphic sites

Lineages	(NS)	(S)	(H)	(Hd)	(Pi)	D de Tajima	p[D ≤ Dt]	R^2	p[R^2 ≤ Ri]
L. antumalguen + *L.* sp. 7	076	056	035	0.9510	0.01029	−1.29419	0.0752	0.0582	0.78600
L. burmeisteri	018	001	002	0.5230	0.09080	1.50518	0.9680	0.2614	0.98305
L. chillanensis	021	024	015	0.9520	0.00959	−0.11134	0.0000	0.1184	0.41100
L. crandalli	036	042	025	0.9710	0.00745	−1.80422	0.0144	0.0513	0.00320
L. elongatus + *L. shitan*	262	134	100	0.9327	0.01366	−1.77024	0.0056	0.0332	0.01380
L. carlosgarini + *L.* sp. 1	060	069	028	0.9570	0.01893	−0.46740	0.3620	0.0908	0.38660
L. smaug	044	037	019	0.9410	0.01218	−0.11458	0.5098	0.1057	0.50880
L. sp. 2	008	003	003	0.6790	0.00196	0.58467	0.7794	0.2099	0.37630
L. sp. 3	007	002	003	0.6670	0.00113	−0.27492	0.5132	0.2116	0.21423
L. sp. 6a	004	002	002	0.5000	0.00148	−0.70990	0.6000	0.4330	1.00000
L. sp. 6b	020	012	009	0.8790	0.00370	−0.94209	0.1800	0.0962	0.09218
L. antumalguen + *L.* sp. 7 + *L.* sp. 6 a y b + *L. chillanensis*	121	098	061	0.9760	0.01943	−0.90916	0.1920	0.0648	0.18420

Its pairwise genetic distances were >4% compared to all other haploclades, but a limited sample size precluded further analyses. It will be necessary to increase sampling in this area to further evaluate the status of this candidate species.

South of the Colorado River in north-western Neuquén province, the landscape is characterized by numerous mountain ranges and deep valleys (Martínez and Kutschker 2011). Here, we identified several haploclades within the *L. elongatus* complex, including *L. carlosgarini*, *L. chillanensis*, (*L. antumalguen* + *L.* sp. 7), *L. burmeisteri*, and *L.* sp. 6a and *L.* sp. 6b. The type locality of *L. carlosgarini* is in Chile but near the Argentinian border (Fig. 1, loc. *3 [locs. 93/105]), and is the

only locality of this haploclade north of the Colorado River (Fig. 1, green triangles). As mentioned above, five of the seven individuals from the type locality of *L. carlosgarini* shared haplotypes within the *L. smaug cyt-b* network (Fig. 3, panel b, yellow *3); the remaining two other individuals were inferred within the *L. carlosgarini* network (in terminal positions; Fig. 3, panel a, orange circles, yellow *3). Taking into account the possible role of the Colorado River as a barrier, the recency of these divergences, and the geographical context of this genetic structure, these shared haplotypes may also be best explained by incomplete lineage sorting. The *cyt-b* gene tree (Fig. 2) inferred one haploclade that included *L.* sp. 1 haplotypes (Fig. 1, loc. *2

[loc. 82]), a candidate species under formal description (Esquerré, personal communication) and those from *L. carlos-garini* haplotypes (Fig. 1, loc. *3 [locs. 93/105]), while the network analyses inferred these two groups as separate networks (Fig. 3, panel a). *Liolaemus* sp. 1 is geographically separated from *L. smaug* and *L. carlosgarini* by cordilleras and valleys and is isolated in the western part of the Andes; thus, it may represent incipient differentiation due to geographic isolation.

Individuals of *L. chillanensis* and *L. antumalguen* (pairwise *cyt-b* distance <4% [2.7%, Table 1]) were all inferred on a single network. The type locality of *L. chillanensis* is in Chile but also close to the Argentinian border (Fig. 1, loc. *6 [loc. 8]). Individuals from the type locality carry two haplotypes (Fig. 3, panel g, purple circles with a black star) that have an intermediate position between the rest of the haplotypes from this species (Fig. 3, panel g, grey shade, separated by seven mutational steps) and those of *L. antumalguen* + *L.* sp. 7 (Fig. 3, panel g, blue shade). In the *KIF24* nuclear networks (Fig. 4, panel c), *L. chillanensis* shares a haplotype with *L. antumalguen*, *L. carlosgarini* and *L.* sp. 6, and in the other network (Fig. 4, panel d), it shares different haplotypes with these species, but it also has unique haplotypes. While the haplotype diversity of *L. chillanensis* is high, the nucleotide diversity is low and less than that of the haploclades distributed north of the Colorado River, which is consistent with the significant signal for deviation from neutrality detected by Tajima's test (Table 2), and the Bayesian skyline plot signal for recent fluctuations in the effective population size. There are two possible explanations for this pattern: 1 – the divergence of these haploclades is very recent and they have not reached reciprocal monophyly with the nuclear markers (Fig. 4, panels c and d); 2 – the non-neutrality detected by the Tajima test (Table 2) and the variation in population size (Fig. S2) are evidence of recent contact and gene flow, also suggested by the connection on the haplotype network (Fig. 3, panel g). Further geographic sampling to include intermediate geographic areas between these species will be needed to clarify their evolutionary histories.

Within the *L. antumalguen* haploclade (Fig. 2) and the *cyt-b* network (Fig. 3, panel g), the three haplotypes from the type locality of this species were inferred to be closely related (Fig. 3, panel g, pink circles with a black star). The original description of this species records it only from its type locality, at 2300 m on Domuyo Volcano. Individuals from the four lower elevation localities we sampled in the area (Fig. 1, locs. 1–4), previously referred to as *L.* sp. 7 (Morando et al. 2003), are linked to the same section of the *L. antumalguen* network (Fig. 3, panel g, blue shade area). The pattern is consistent with a model of peripatric speciation in which *L. antumalguen* may have been originated as a peripheral lineage isolated on this peak. The most likely 'source' population may have been the immediate ancestor of *L.* sp. 7, as suggested by this candidate species' larger altitudinal range (1550–2250 m), and the paraphyletic structure of its mtDNA gene tree. Morphologically, these two taxa have a marked cline on their overall size and colour pattern (Avila et al. 2010). The *L. antumalguen* network also included one haplotype shared between two individuals from the type locality of *L. choique* (Fig. 3, panel g, blue circle with a red *4), highlighting the need to include more individuals and high-resolution nuclear markers (e.g. SNP data) to disentangle the complex evolutionary history of these lineages.

Further south of the distribution of *L. antumalguen* and *L. chillanensis*, are localities assigned to *L.* sp. 6 (Fig. 1, locs 108-13, yellow triangles), proposed as a candidate species by Morando et al. (2003) for localities 108 and 112. In the *cyt-b* tree *L. antumalguen* and *L. chillanensis* were inferred as closely

related to *L.* sp. 6 with high statistical support (PP = 1, Fig. 2), but *L.* sp. 6 was not monophyletic; some *L.* sp. 6 haplotypes formed separate networks (Fig. 3, panel c), and were placed in different parts of *12S* (Fig. 4, panel a) and the nuclear multilocus networks (Fig. 4, panel d). With the two nuclear markers, *L.* sp. 6 had shared haplotypes with *L. antumalguen* and *L. chillanensis* (and *L. carlosgarini*) (Fig. 4, panels c and d). Also, *L.* sp. 6 (a and b) had pairwise genetic distances <4% versus these species. Again, higher resolution multilocus data will be needed to clearly understand these closely related taxa within this complex.

Within this same north-western Patagonian region (north-western Neuquén), is the type (and only known) locality of *L. burmeisteri*, whose haplotypes were inferred as a clade with high support in the *cyt-b* tree (PP = 1, Fig. 2), and as a separate network (Fig. 3, panel f). Nuclear genes also showed evidence that this lineage is the most differentiated of the complex; it had unique haplotypes not integrated into the networks (Fig. 4, panels c and d). All evidence indicates an independent evolutionary history for this taxon, but the small sample size precluded further detailed analyses.

The Protected Natural Area (PNA) Auca Mahuida (Fig. 1, locs. 14–16 in north-eastern Neuquén Province) includes several volcanoes, one that gives the area its name. Topographically the altitude ranges from 223 m up to 2258 m, the highest peak being on the Auca Mahuida volcano. This area is isolated from the Cordillera de los Andes, and all published evidence to date indicates that the lizard populations on these volcanoes are also isolated (Avila et al. 2011, 2013b; Martínez and Kutschker 2011). Our more inclusive samples from the PNA region are all linked in the *L. crandalli* haploclade (Fig. 2, PP = 1), with pairwise genetic distances with other lineages >4% (except vs. *L.* sp. 3; Table 1). These halplotypes also form a separate *cyt-b* network (Fig. 3, panel i) and had unique nuclear haplotypes (Fig. 4, panels c and d), consistent with a history of isolation for *L. crandalli*.

Individuals from Pino Hachado locality in Neuquén province (Fig. 1, loc. 107), close to the northern edge of the distribution of *L. elongatus*, form a distinct haploclade (PP = 1) sister to *L. elongatus* (PP = 1), which we named *L.* sp. 3 (Fig. 2). Our mitochondrial (Figs. 2; 3, panel e) and nuclear data (Fig. 4, panels c and d) indicate that these individuals are different from *L. elongatus*; they have unique haplotypes for all loci, but again our small sample size precluded further phylogeographic inferences.

The (*L. elongatus* + *L. shitan*) haploclade is southernmost distributed in the *L. elongatus* complex (Fig. 1, blue circles), with *cyt-b* haplotypes from the type locality of *L. shitan* (Fig. 1, *9 [loc. 65]) interdigitated with those from the rest of the distribution of *L. elongatus* (Fig. 2). In older literature, the distribution of *L. elongatus* was interpreted to extend from southern Chubut to the provinces of Catamarca and La Rioja, but Morando et al. (2003) noted that the range of this species most likely would be limited to south of the Agrio River in central Neuquén. During the last decade, several new species have been described in the northern areas of Neuquén and Mendoza (Avila et al. 2010, 2011, 2012; Abdala et al. 2012a,b), and a recent review on the geographic distribution of this species (Minoli et al. 2013) proposed a distribution for *L. elongatus sensu stricto* concordant with what we propose in this study (Fig. 1, blue circles). In the *cyt-b* tree, this haploclade was inferred with high support (Fig. 2, PP = 1), and it is also a separate network (Fig. 3, panel g) that includes haplotypes from the *L. shitan* type locality in terminal positions (Fig. 3, panel g, three purple circles with black stars). The nuclear genes also do not resolve differences between *L. elongatus* and *L. shitan*; some haplotypes are shared with

L. antumalguen, two are closely related to *L. burmeisteri* and one to *L. carlosgarini* (Fig. 4, panels c and d). The geographic range of this haploclade is the largest in the complex (Fig. 1); it includes the largest number of localities and sequences, and the highest number of polymorphic sites and haplotypes of the complex (Table 2). Both neutrality tests had significant results (Table 2), and the BSP graph analysis (Fig. S2) showed a change in the effective population size over time, strongly suggesting a recent range and/or population expansion, most possibly towards the southern end of its range.

Although we present the most detailed geographic and individual sampling scheme in terms of populations and markers for this complex, our results show that it is still necessary to increase sampling in some areas, and to include dozens of hundreds of high-resolution nuclear markers (e.g. SNPs) to resolve the evolutionary and demographic histories of these lineages. Our results suggest that these histories may have been very complex, and were likely driven by Pleistocene climate cycles on an extremely topographically diverse landscape (Rabassa et al. 2005). These successive climate cycles almost certainly drove repeated periods of population isolation and expansion, some of which likely involved secondary contact or reinforcement.

Taxonomic implications

Molecular analyses of the *L. elongatus* complex clearly differentiated *L. burmeisteri*, *L. crandalli*, *L. chillanensis*, *L.* sp. 2 and *L.* sp. 3; these lineages also show morphological differences among themselves and with other species (Medina 2015), supporting their specific status. Although this evidence does not allow molecular distinction between *L. elongatus* and *L. shitan*, they show morphological distinction between individuals from type localities (Medina 2015). Other nominal taxa show various patterns of haplotype sharing that present a challenge for species delimitation: (1) *L. carlosgarini* is not clearly differentiated from *L.* sp. 1 and *L. smaug*, but morphological differences have been detected among these three taxa (Medina 2015), (2) *L. antumalguen* is not independent from *L.* sp. 7, but they present morphological differences (Medina 2015). These two cases may represent recent lineage divergences with incomplete lineage sorting or some level of gene flow, for which other kinds of data (e.g. SNP, morphology) are needed to test these species hypotheses. *Liolaemus choique* does not have any exclusive haplotype, and it is inferred within the *L. smaug* and *L. antumalguen* + *L.* sp. 7 haploclades; thus, our molecular evidence does not support its specific status. For the candidate species *L.* sp. 6 (here inferred as two clades, a and b), our results are consistent with a degree of incipient differentiation from the other taxa, but more studies are needed to test its candidate species status. In summary, our results present evidence with different degrees of support, for the recognition of most of the species previously described for the *L. elongatus* complex: *L. antumalguen*, *L. chillanensis*, *L. carlosgarini*, *L. burmeisteri*, *L. smaug*, *L. elongatus* and *L. crandalli* and four candidate species (*L.* sp. 1, *L.* sp. 2, *L.* sp. 3 and *L.* sp. 7); the evidence is insufficient to assess the status of *L.* sp. 6 and does not support *L. choique* and *L. shitan*. Even more, different lines of evidence summarized within an integrative taxonomy approach (de Queiroz 2005; Padial and De la Riva 2007; Padial and De La Riva 2009; Aguilar et al. 2013, 2016) will shed light for the status of previous or new candidate species.

The exclusive analysis of mitochondrial genomes in phylogeographic studies may provide misleading depictions of the species tree (Brito and Edwards 2009), but this limitation is recognized and there is an increasing use of multiple nuclear markers in phylogeographic studies of many types of organisms (Hackett

et al. 2008; Stöck et al. 2008; Camargo et al. 2012b). These multilocus studies avoid biases associated with mitochondrial loci and can accommodate nuclear gene tree heterogeneity that might result from incomplete lineage sorting, interspecific gene flow, estimation error or mutational stochasticity (Pamilo and Nei 1988; Avise 1989; Maddison 1997). This is now a preferred approach for reconstructing the evolutionary history of closely related populations or species (Markolf et al. 2011). Because all of this, it will be necessary to incorporate other genomic markers and a comprehensive morphological set (Aguilar et al. 2016) to delimit species limits and infer evolutionary relationships of the *L. elongatus* complex.

Acknowledgements

References

Abdala CS, Quinteros AS (2014) Los últimos 30 años de estudios de la familia de lagartijas más diversa de Argentina. Actualización taxonómica y sistemática de Liolaemidae. Cuad Herpetol **28**:55–82.

Abdala CS, Quinteros AS, Scrocchi GJ, Stazzonelli JC (2010) Three new species of the *Liolaemus elongatus* group (Iguania: Liolaemidae) from Argentina. Cuad Herpetol **24**:2.

Abdala CS, Acosta JL, Acosta JC, Álvarez BB, Arias F, Avila LJ, Blanco MG, Bonino M, Boretto JM, Brancatelli G (2012a) Categorización del estado de conservación de las lagartijas y anfisbenas de la República Argentina. Cuad Herpetol **26**:215–247.

Abdala CS, Semhan RV, Moreno Azocar DL, Bonino M, Paz MM, Cruz F (2012b) Taxonomic study and morphology based phylogeny of the patagonic clade *Liolaemus melanops* group (Iguania: Liolaemidae), with the description of three new taxa. Zootaxa **3163**:1–32.

Aguilar C, Wood PL Jr, Cusi JC, Guzmán A, Huari F, Lundberg M, Mortensen E, Ramírez C, Robles D, Suárez J, Ticona A, Vargas VJ, Venegas PJ, Sites JW Jr (2013) Integrative taxonomy and preliminary assessment of species limits in the *Liolaemus walkeri* complex (Squamata, Liolaemidae) with descriptions of three new species from Peru. ZooKeys **364**:47–91.

Aguilar C, Wood . PL Jr, Belk M, Duff MH, Sites JW Jr (2016) Different roads lead to Rome: Integrative taxonomic approaches lead to the discovery of two new lizard lineages in the *Liolaemus montanus* group (Squamata: Liolaemidae). Biol J Linn Soc DOI: 10.1111/bij.12890.

Avila LJ, Morando M, Perez CHF, Sites JW Jr (2004) Phylogenetic relationships of lizards of the *Liolaemus petrophilus* group (Squamata, Liolaemidae), with description of two new species from western Argentina. Herpetologica **60**:187–203.

Avila LJ, Morando M, Pérez D, Sites JW Jr (2010) A new species of the *Liolaemus elongatu*s clade (Reptilia: Iguania: Liolaemini) from Cordillera del Viento, northwestern Patagonia, Neuquén, Argentina. Zootaxa **2667**:28–42.

Avila LJ, Pérez CHF, Pérez DR, Morando M (2011) Two new mountain lizard species of the *Phymaturus* genus (Squamata: Iguania) from northwestern Patagonia, Argentina. Zootaxa **2924**:1–21.

Avila LJ, Pérez CHF, Medina CD, Sites JW Jr, Morando M (2012) A new species lizard of the *Liolaemus elongatus* clade (Squamata: Iguania: Liolaemini) from Curi Leuvu River Valley, northern Patagonia, Neuquén, Argentina. Zootaxa 3325:37–52.

Avila LJ, Martinez LE, Morando M (2013a) Checklist of lizards and amphisbaenians of Argentina: an update. Zootaxa 3616:201–238.

Avila LJ, Olave M, Pérez CHF, Perez DR, Morando M (2013b) Molecular phylogenetic relationships of the *Liolaemus rothi* complex and a new species of lizard from Auca Mahuida Volcano (Squamata: Liolaemini). Zootaxa 3608:221–238.

Avila LJ, Medina CD, Perez CHF, Sites JW Jr, Morando M (2015) Molecular phylogenetic relationships of the *Liolaemus elongatus* clade (Iguania: Liolaemini) and a new species of lizard from an isolated volcanic peak in northern Patagonia. Zootaxa 3947:67–84.

Avise JC (1989) Gene trees and organismal histories: a phylogenetic approach to population biology. Evolution 43:1192–1208.

Breitman MF, Avila LJ, Sites JW Jr, Morando M (2012) How lizards survived blizzards: phylogeography of the *Liolaemus lineomaculatus* group (Liolaemidae) reveals multiple breaks and refugia in southern Patagonia and their concordance with other codistributed taxa. Mol Ecol 21:6068–6085.

Breitman MF, Minoli I, Avila LJ, Medina CD, Sites JW Jr, Morando M (2014) Lagartijas de la provincia de Santa Cruz, Argentina: distribution geográfica, diversidad genética y estado de conservación. Cuad Herpetol 28:83–110.

Brito PH, Edwards SV (2009) Multilocus phylogeography and phylogenetics using sequence-based markers. Genetica 135:439–455.

Camargo A, Avila LJ, Morando M, Sites JW Jr (2012a) Accuracy and precision of species trees: effects of locus, individual, and base pair sampling on inference of species trees in lizards of the *Liolaemus darwinii* group (Squamata, Liolaemidae). Syst Biol 61:272–288.

Camargo A, Morando M, Avila LJ, Sites JW Jr (2012b) Species delimitation with ABC and other coalescent-based methods: a test of accuracy with simulations and an empirical example with lizards of the *Liolaemus darwinii* complex (Squamata: Liolaemidae). Evolution 66:2834–2849.

Casagranda MD, Roig-Juñent S, Szumik C (2009) Endemismo a diferentes escalas espaciales: un ejemplo con Carabidae (Coleoptera: Insecta) de América del Sur austral. Rev Chilena Hist Nat 82:17–42.

Cei JM (1986) Reptiles del centro, centro-oeste y sur de la Argentina. Mus Reg di Scienze Nat Torino, Monografie 4:1–527.

Cei JM (1993) Reptiles del noroeste, nordeste y este de la Argentina. Mus Reg di Scienze Nat Torino, Monografie 14:1–949.

Chehébar C, Novaro A, Iglesias G, Walker S, Funes M, Tammone M, Didier K (2013) Identificación de áreas de importancia para la biodiversidad en la estepa y el monte de Patagonia. ErreGé & Asociados. https://www.sib.gov.ar/archivos/Pub_APN_WCS_TNC2013.pdf

Clement M, Posada D, Crandall KA (2000) TCS: a computer program to estimate gene genealogies. Mol Ecol 9:1657–1659.

Corbalán V, Tognelli MF, Scolaro JA, Roig-Juñent SA (2011) Lizards as conservation targets in Argentinean Patagonia. J for Nat Conserv 19:60–67.

Darriba D, Taboada GL, Doallo R, Posada D (2012) jModelTest 2: more models, new heuristics and parallel computing. Nat Methods 9:772.

Díaz Gómez JM, Lobo F (2006) Historical biogeography of a clade of *Liolaemus* (Iguania: Liolaemidae) based on ancestral areas and dispersal-vicariance analysis (DIVA). Papéis Avulsos de Zoologia (São Paulo) 46:261–274.

Domínguez MC, Roig-Juñent S, Tassin JJ, Ocampo FC, Flores GE (2006) Areas of endemism of the Patagonian steppe: an approach based on insect distributional patterns using endemicity analysis. J Biogeography 33:1527–1537.

Donoso Barros R (1966) Reptiles de Chile. Ediciones de la Universidad de Chile Santiago, Chile.

Drummond AJ, Rambaut A (2007) BEAST: Bayesian evolutionary analysis by sampling trees. BMC Evol Biol 7:214.

Esquerré D, Núñez H, Scolaro JA (2013) *Liolaemus carlosgarini* and *Liolaemus riodamas* (Squamata: Liolaemidae), two new species of lizards lacking precloacal pores, from Andean areas of central Chile. Zootaxa 3619:428–452.

Etheridge R (1995) Redescription of *Ctenoblepharis adspersa* Tschudi, 1845, and the taxonomy of Liolaemidae (Reptilia, Squamata, Tropiduridae). Am Mus Novit 3142:1–34.

Etheridge R, Espinoza R (2000) Taxonomy of the Liolaeminae (Squamata: Iguania: Tropiduridae) and a semi-annotated bibliography. Smithson Herpetol Inf Serv 126:64.

Excoffier L, Laval G, Schneider S (2005) Arlequin (version 3.0): an integrated software package for population genetics data analysis. Evol Bioinform 1:47.

Feltrin N (2013) Conservadurismo o divergencia de nicho filogenético: especies patagónicas del grupo *petrophilus* (Squamata: *Liolaemus*) como caso de estudio. PhD Thesis, Universidad Nacional de Córdoba, Córdoba.

Fontanella FM, Olave M, Avila LJ, Sites JW Jr, Morando M (2012) Molecular dating and diversification of the South American lizard genus *Liolaemus* (subgenus *Eulaemus*) based on nuclear and mitochondrial DNA sequences. Zool J Linn Soc 164:825–835.

Fouquet A, Gilles A, Vences M, Marty C, Blanc M, Gemmell NJ (2007) Underestimation of species richness in Neotropical frogs revealed by mtDNA analyses. PLoS ONE 2:e1109.

Guindon S, Gascuel O (2003) A simple, fast and accurate method to estimate large phylogenies by maximum-likelihood. Syst Biol 52:696–704.

Hackett SJ, Kimball RT, Reddy S, Bowie RCK, Braun EL, Braun MJ, Chojnowski JL, Cox WA, Han K-L, Harshman J, Huddleston CJ, Marks BD, Miglia KJ, Moore WS, Sheldon FH, Steadman DW, Witt CC, Yuri T (2008) A phylogenomic study of birds reveals their evolutionary history. Science 320:1763–1768.

Harmon LJ, Schulte JA II, Larson A, Losos JB (2003) Tempo and mode of evolutionary radiation in iguanian lizards. Science 301:961–964.

Heath L, Van der Walt E, Varsani A, Martin D (2006) Recombination patterns in aphthoviruses mirror those found in other picornaviruses. J Virol 80:11827–11832.

Huelsenbeck JP, Ronquist F (2001) MrBayes: Bayesian inference of phylogeny. Bioinformatics 17:754–755.

Huson DH, Bryant D (2005) Application of phylogenetic networks in evolutionary studies. Mol Biol Evol 23:254–267.

Joly S, Bruneau A (2006) Incorporating allelic variation for reconstructing the evolutionary history of organisms from multiple genes: an example from *Rosa* in North America. Syst Biol 55:623–636.

Kass RE, Raftery AE (1995) Bayes factors. JASA 90:773–795.

Laurent RF (1983) Contribución al conocimiento de la estructura taxonómica del género *Liolaemus* Wiegmann (Iguanidae). Boletín de la Asociación Herpetológica Argentina 1:15–18.

Leaché AD, Koo MS, Spencer CL, Papenfuss TJ, Fisher RN, McGuire JA (2009) Quantifying ecological, morphological, and genetic variation to delimit species in the coast horned lizard species complex (*Phrynosoma*). PNAS 106:12418–12423.

Librado P, Rozas J (2009) DnaSP v5: a software for comprehensive analysis of DNA polymorphism data. Bioinformatics 25:1451–1452.

Lobo F, Nenda SJ (2015) Discovery of two new species of *Phymaturus* (Iguania: Liolaemidae) from Patagonia, Argentina, and occurrence of melanism in the *patagonicus* group. Cuad Herpetol 29:5–25.

Lobo F, Espinoza RE, Quinteros AS (2010) A critical review and systematic discussion of recent classification proposals for liolaemid lizards. Zootaxa 2549:1–30.

Maddison WP (1997) Gene trees in species trees. Syst Biol 46:523–536.

Markolf M, Brameier M, Kappeler PM (2011) On species delimitation: yet another lemur species or just genetic variation? BMC Evol Biol 11:216.

Martin D, Rybicki E (2000) RDP: detection of recombination amongst aligned sequences. Bioinformatics 16:562–563.

Martínez LE (2012) Métodos empíricos para delimitar especies: el complejo *Liolaemus bibronii* (Squamata: Liolaemini) como ejemplo. PhD Thesis, Universidad Nacional de Córdoba, Córdoba.

Martínez OA, Kutschker A (2011) The 'Rodados Patagónicos' (Patagonian shingle formation) of eastern Patagonia: environmental conditions of gravel sedimentation. Biol J Linn Soc 103:336–345.

Medina CD (2015) Estudio sistemático de los complejos de lagartijas patagónicas *Liolaemus elongatus* y *L. kriegi* (Squamata: *Liolaemus*). PhD Thesis, Universidad Nacional de Córdoba, Córdoba.

Medina CD, Avila LJ, Morando M (2013) Hacia una taxonomía integral: poniendo a prueba especies candidatas relacionadas a *Liolaemus buergeri* Werner 1907 (Iguania: Liolaemini) mediante análisis morfológicos. Cuad Herpetol **27**:27–34.

Medina CD, Avila LJ, Sites JW Jr, Morando M (2014) Multilocus phylogeography of the Patagonian lizard complex *Liolaemus kriegi* (Iguania: Liolaemini). Biol J Linn Soc **113**:256–269.

Minoli I, Medina CD, Frutos N, Morando M, Avila LJ (2013) A revised geographical range for *Liolaemus elongatus* Koslowsky, 1896 (Squamata: Liolaemini) in Argentina: review of reported and new-data based distribution with new localities. Acta Herpetologica **8**:159–162.

Morando M, Avila LJ, Sites JW Jr (2003) Sampling strategies for delimiting species: Genes, individuals, and populations in the Liolaemus elongatus-kriegi complex (Squamata: Liolaemidae) in Andean-Patagonian South America. Syst Biol **52**:159–185.

Morando M, Avila LJ, Baker J, Sites JW Jr (2004) Phylogeny and phylogeography of the *Liolaemus darwinii* complex (Squamata: Liolaemidae): evidence for introgression and incomplete lineage sorting. Evolution **58**:842–861.

Morando M, Avila LJ, Turner CR, Sites JW Jr (2007) Molecular evidence for a species complex in the patagonian lizard *Liolaemus bibronii* and phylogeography of the closely related *Liolaemus gracilis* (Squamata: Liolaemini). Mol Phylogenet Evol **43**:952–973.

Morando M, Avila LJ, Perez CHF, Hawkins MA, Sites JW Jr (2013) A molecular phylogeny of the lizard genus *Phymaturus* (Squamata, Liolaemini): implications for species diversity and historical biogeography of southern South America. Mol Phylogenet Evol **66**:694–714.

Noonan PB, Yoder AE (2009) Anonymous nuclear markers for Malagasy plated lizards (*Zonosaurus*). Mol Ecol Resour **9**:402–404.

Olave M, Martinez LE, Avila LJ, Sites JW Jr, Morando M (2011) Evidence of hybridization in the Argentinean lizards *Liolaemus gracilis* and *Liolaemus bibronii* (Iguania: Liolaemini): an integrative approach based on genes and morphology. Mol Phylogenet Evol **61**:381–391.

Olave M, Avila LJ, Sites JW Jr, Morando M (2017) Hidden diversity within the lizard genus *Liolaemus*: Genetic vs morphological divergence in the *L. rothi* complex (Squamata: Liolaeminae). Mol Phylogenet Evol **107**:56–63.

Padial JM, De la Riva I (2007) Taxonomic inflation and the stability of species lists: the perils of Ostrich's Behavior. Syst Biol **55**:859–867.

Padial JM, De La Riva I (2009) Integrative taxonomy reveals cryptic Amazonian species of *Pristimantis* (Anura: Strabomantidae). Zool J Linn Soc **155**:97–122.

Pamilo P, Nei M (1988) Relationships between gene trees and species trees. Mol Biol Evol **5**:568–583.

Pincheira-Donoso D, Scolaro JA, Sura P (2008) A monographic catalogue on the systematics and phylogeny of the South American iguanian lizard family Liolaemidae (Squamata, Iguania). Zootaxa **1800**:1–85.

Pincheira-Donoso D, Hodgson DJ, Stipala J, Tregenza T (2009) A phylogenetic analysis of sex-specific evolution of ecological morphology in *Liolaemus* lizards. Ecol Res **24**:1223–1231.

Pond SLK, Muse SV (2005) HyPhy: Hypothesis Testing Using Phylogenies. Statistical Methods in Molecular Evolution. Springer, New York, pp 125–181.

Portik DM, Wood PL, Grismer JL, Stanley EL, Jackman TR (2011) Identification of 104 rapidly-evolving nuclear protein-coding markers for amplification across scaled reptiles using genomic resources. Conserv Genet Resour **4**:1–10.

de Queiroz K (2005) A Unified Concept of Species and Its Consequences for the Future of Taxonomy. Proc Calif Acad Sci **56**:196–215.

Rabassa J, Clapperton CM (1990) Quaternary glaciations of the southern Andes. Quat Sci Rev **9**:153–174.

Rabassa J, Coronato AM, Salemme M (2005) Chronology of the Late Cenozoic Patagonian glaciations and their correlation with biostratigraphic units of the Pampean region (Argentina). J South Am Earth Sci **20**:81–103.

Rambaut A, Drummond AJ (2009) Tracer v1.4, Available from http://beast.bio.ed.ac.uk/Tracer.

Ramos VA, Folguera A (2011) Payenia volcanic province in the Southern Andes: an appraisal of an exceptional Quaternary tectonic setting. J Vol Geo Res **201**:53–64.

Ramos VA, Ghiglione MC (2008) Tectonic evolution of the patagonian andes. Develop Quaternary Sci **11**:57–71.

Ramos VA, Kay S (2006) Overview of the tectonic evolution of the southern Central Andes of Mendoza and Neuquén (35–39 S latitude). In: Basu A, Bickford ME (eds), Evolution of an Andean Margin: A Tectonic and Magmatic View from the Andes to the Neuquén Basin (35 Degrees-39 Degrees S Lat). The Geological Society of America Inc, Colorado, USA.

Ramos-Onsins SE, Rozas J (2002) Statistical properties of new neutrality tests against population growth. Mol Biol Evol **19**:2092–2100.

Ronquist F, Huelsenbeck JP (2003) Mr Bayes 3: Bayesian phylogenetic inference under mixed models. Bioinformatics **19**:1572–1574.

Schulte JA II, Macey JR, Espinoza RE, Larson A (2000) Phylogenetic relationships in the iguanid lizard genus *Liolaemus*: multiple origins of viviparous reproduction and evidence for recurring Andean vicariance and dispersal. Biol J Linn Soc **69**:75–102.

Sérsic AN, Cosacov A, Cocucci AA, Jonson LA, Pozner R, Avila LJ, Sites JW Jr, Morando M (2011) Emerging phylogeographical patterns of plants and terrestrial vertebrates from Patagonia. Biol J Linn Soc **103**:475–494.

Stöck M, Dubey S, Klütsch C, Litvinchuk SN, Scheidt U, Perrin N (2008) Mitochondrial and nuclear phylogeny of circum-Mediterranean tree frogs from the *Hyla arborea* group. Mol Phylogenet Evol **49**:1019–1024.

Tajima F (1989) The effect of change in population size on DNA polymorphism. Genetics **123**:597–601.

Torres-Pérez F, Méndez MA, Benavides E, Moreno RA, Lamboroto M, Palma RE, Ortiz JC (2009) Systematics and evolutionary relationships of the mountain lizard *Liolaemus monticola* (Liolaemini): how morphological and molecular evidence contributes to reveal hidden species diversity. Biol J Linn Soc **96**:635–650.

Supporting Information

Additional Supporting Information may be found in the online version of this article:

Figure S1. Concatenated mitochondrial gene network.

Figure S2. Bayesian skyline plot graphs.

Table S1. Sampling of specimens – Geographic Information.

Table S2. Sampling of species and individuals – GenBank accession numbers for *cyt-b*.

Table S3. Sampling of species and individuals – GenBank accession numbers for *12S, KIF24* and *LDAB1D* genes.